Final Report
NASA Grant NAG-3-2419
1 May 2003 – 13 February 2004

Measurement of Turbulent Pressure and Temperature Fluctuations in a Gas Turbine Combustor

Submitted to:
NASA Glenn Research Center
Technical Officer: Louis Povinelli
Grant Administrator: Heidi Shaw

Submitted By:
John E.LaGraff (Syracuse University)
Cristina Bramanti (Centrospazio, Pisa, Italy)
Martin Oldfield (Oxford University, Oxford, UK)
Andrea Passaro (Centrospazio, Pisa, Italy)
Leonardo Biagioni (Centrospazio, Pisa, Italy)

13 March 2004

ABSTRACT

The report summarizes the results of the redesign efforts directed towards the gas-turbine combustor rapid-injector flow diagnostic probe developed under sponsorship of NASA-GRC and earlier reported in NASA-CR-2003-212540. Lessons learned during the theoretical development, developmental testing and field-testing in the previous phase of this research were applied to redesign of both the probe sensing elements and of the rapid injection device. This redesigned probe (referred to herein as Turboprobe) has been fabricated and is ready, along with the new rapid injector, for field-testing. The probe is now designed to capture both time-resolved and mean total temperatures, total pressures and, indirectly, one component of turbulent fluctuations.

1. Introduction

The field test carried out in the ENEL combustor facility with the Turboprobe mechanism and reported in Ref.1, led to several ideas for improving performance characteristics.

The first redesign effort focused on the analysis of the injection mechanism in order to control the valves separately and enabling the use of bottled nitrogen to power the injections (in particular, plumbing the cylinder from the atmosphere). The second effort focused on the design of a single probe head with multiple sensors for attaining a better knowledge of the turbulent fluctuations in the exit flow of a gas turbine combustor, providing wide bandwidth, simultaneous temperature measurements of on a single, field-replaceable probe.

First, the new valve control and the main experimental results validating its performances are presented. Then the redesign and final calibration of the new probe are illustrated. An additional circuit designed to measure the Kulite current, and hence the Kulite temperature, is also described.

The injector redesign effort was centred at Pisa (Centrospazio Space Research Laboratory) and the probe redesign in Oxford.

Finally, the modified design Turboprobe mechanism (metric version), mounted in the new access ENEL-Sesta port, is shown in preparation for a possible future field-test.

2. Injection valve control description

The first step in the development of Turboprobe injection characteristics was to enable the use of a nitrogen bottle inside the ENEL-Sesta rig area by modifying the valve control in order to obtain a lower air bottle consumption (in fact, during the last tests it was esteemed that one 200 bar nitrogen bottle would allow about 45 minutes of operation in nominal conditions, which is clearly not satisfactory for that utilization).

The idea was to separate the valve control (the intake ones from the exhaust ones) and to connect all the valves to the air bottle (previously all the valves were controlled by the same signal pulse and only two valves were connected to the air bottle).

To achieve this new requirement it was essential to analyze the DAQ board characteristics, in order to examine the possibility of assigning one digital channel as well as a counter (to count the time-ticks and to control the effective pulse delay and pulse width for the injection) to each relay. After checking it out, and finding an appropriate solution to the problem, all the new electrical connections inside the DAQ board were modified as well as the original Labview program for injection control [2].

At this time the valves are controlled separately by two different relays through the new Labview program and it's now possible to control the pulse delay and the pulse width of each couple of valves as well as the 3 injection phases (injection, stationary time at maximum distance, retract).

Table1 presents the valve plumbing details of the present probe system configuration and Figure1 shows the new separated control valves scheme.

Valve	A	R	P
1	F	Open Air	Bottle
2	F	Open Air	Bottle
3	R	Open Air	Bottle
4	R	Open Air	Bottle

Table1. Plumbing details for the injector valves.

SYRACUSE UNIVERSITY

OFFICE OF SPONSORED PROGRAMS

April 28, 2004

NASA Center for Aerospace Information (CASI)
Attn: Document Processing Section
7121 Standard Drive
Hanover, MD 21076

RE: Final Technical Report for Award NAG3-2419
PI: LaGraff, John E.

Enclosed please find one copy of Dr. LaGraff's Final Technical Report for Award NAG3-2419.

If you have any questions regarding this matter, please contact me.

Sincerely,

Stuart Taub
Associate Director
315.443.9356
staub@syr.edu

Enclosures

cc: Grants Office/NASA Glenn Research Center
S. LaPlante/ONR
Louis A. Povinelli/NASA MS 5-3

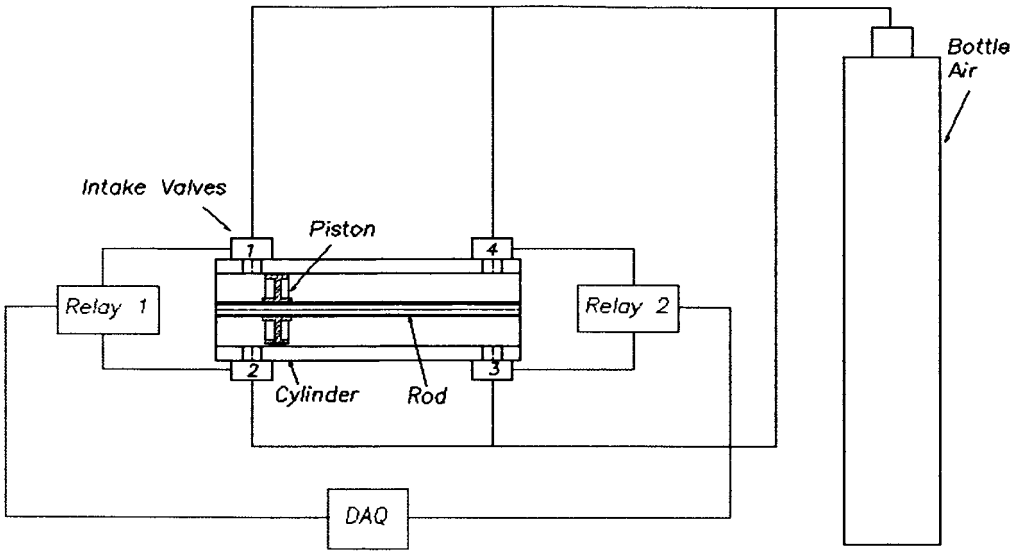

Figure 1.Turboprobe separated injector valve control scheme.

In particular, after more than 250 runs in the new configuration the bottle air consumption is extremely reduced: the new estimate for air consumption is that a bottle should last for over 1250 injections, and for an undefined amount of time at rest, because of the completely closed system with respect to the atmosphere.

3. Injection experimental tests

3.1 Injection test description

With the new valve control configuration, it was necessary to characterize the injection performances which fulfilled the Turboprobe requirements. At first, the main objective was to validate the system and to estimate the best injection conditions, through several preliminary experimental tests which were carried out at variable cylinder pressures and pulse widths. After one hundred and half runs it was possible to determine the best valve control configuration (pulse delay and pulse width for each couple of valves) for three different bottle operative pressures (4, 5, 6 bar).

The results obtained through these experiments allowed to define an "upgraded" test programme in order to investigate more specifically the influence of the pressure and the piston rod weight on the injection performances. In particular, the rod weight was varied by two different amounts, by attaching weights to the end of the probe rod. Table 2 shows the weight summary including also the nominal weight of the piston-rod assembly.

N°	Weight [g]
Nominal weight	102.3
Additional weight # 1	251.9
Additional weight # 2	354.1

Table 2. Different weights on the probe rod

The test conditions analyzed in the "upgraded" experimental programme are available in the next table: test conditions of interest are labelled with letters (A, B, C ...).

Condition	Run	Cylinder Pressure	Buffer Size	Weight	Scan Rate	Pulse Delay 1	Pulse Width 1	Pulse Delay 2	Pulse Width 2
N°	N°	(bar)	(-)	(g)	(Hz)	(s)	(s)	(s)	(s)
A	1-4	4	9000	102.3	100000	0.01	0.035	0.005	0.04
B	5-8	4	8600	102.3	100000	0.01	0.035	0.001	0.04
C	9-12	4	9500	102.3	100000	0.015	0.035	0.005	0.04
D	13-16	4	9100	102.3	100000	0.015	0.035	0.001	0.04
E	17-20	5	9000	102.3	100000	0.01	0.035	0.005	0.04
F	21-24	5	8600	102.3	100000	0.01	0.035	0.001	0.04
G	25-28	5	9500	102.3	100000	0.015	0.035	0.005	0.04
H	29-32	5	9100	102.3	100000	0.015	0.035	0.001	0.04
I	33-36	6	9500	102.3	100000	0.015	0.035	0.005	0.04
L	37-40	6	9100	102.3	100000	0.015	0.035	0.001	0.04
M	41-44	6	10000	102.3	100000	0.015	0.04	0.005	0.04
N	45-48	6	9600	102.3	100000	0.015	0.04	0.001	0.04
O	49-52	4	9500	354.2	100000	0.015	0.035	0.005	0.04
P	53-56	4	9100	354.2	100000	0.015	0.035	0.001	0.04
Q	57-60	4	10500	456.4	100000	0.015	0.035	0.005	0.05
R	61-64	4	10100	456.4	100000	0.015	0.035	0.001	0.05

Table 3. Summary of test conditions

3.2 Injection test results

As previously mentioned, the experimental tests were carried out under several conditions and in this section the main results are presented.

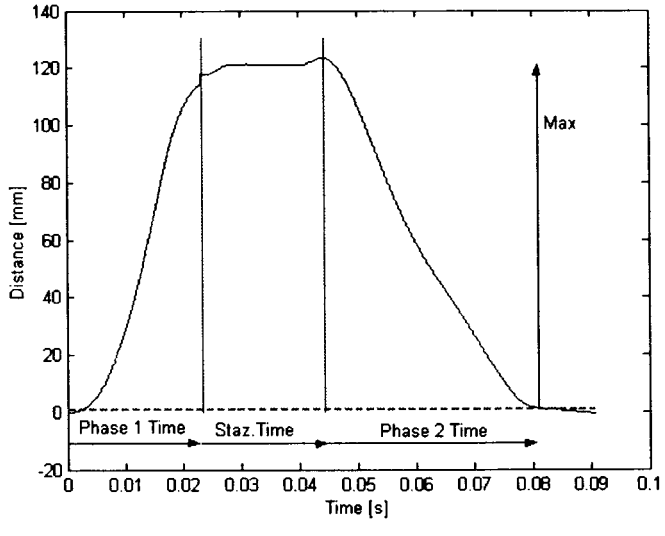

Figure 2. Example of the Turboprobe performance for run n°37

Figure 2 shows the performance characteristics of the injection mechanism, which were measured and represented for each run, in particular:

- the insertion time and speed (phase1)
- the retraction time and speed (phase 2)
- stationary time around maximum penetration (staz)
- the maximum injection distance (Max)
- the total travel time (flowtime)

The time of immersion in the hot flow, or, more importantly for probe survival, the time during which the probe is outside the protective shield, is about 10 ms shorter than the total flowtime (shield distance is about 20 mm).

The next table illustrates the mean values of the performance characteristics for the different conditions presented in table 3. (Herewith only the most interesting and "more effective" results).

Condition N°	Average Max (mm)	Std. Dev. (Max) (mm)	Average Flow Time (ms)	Average Phase1 Time (ms)	Average Phase2 Time (ms)	Average Staz Time (ms)	Average Phase1 Speed (m/s)	Average Phase2 Speed (m/s)
C	112.5	0.58	83.1	29.4	39.6	14.1	3.8	2.84
D	112.5	0.34	85.6	29.4	42.1	14.1	3.81	2.67
G	115.7	0.85	78.9	27.8	36.2	14.9	4.13	3.19
H	115.6	0.63	76.5	27.7	35.7	13	4.15	3.24
I	119.2	0.48	77.2	23.3	33.4	20.5	4.95	3.57
L	118.9	0.34	76.6	20.8	34.4	21.5	5.44	3.47
O	112.2	1.06	90.1	32.5	50	7.63	3.46	2..2
P	112.7	1.10	86.9	31.2	47.3	8.33	3.61	2.25
Q	115.7	1.30	93.1	38.1	52.9	2.12	3.03	2.19
R	115.8	0.98	87.1	38.4	47.4	1.36	3.01	2.44

Table 4. Average performances of the Turboprobe mechanism for several conditions.

It can be noted how, if we observe that the probe is inside the shield on the insertion and retraction for 20 mm, the flowtime is less than 70 ms for all the conditions. The original requirements of 100 mm of immersion distance in 100 ms are completely satisfied. The immersion speed is higher than the retraction one: when the run starts the piston travels toward a zone at atmospheric pressure while when it comes back it has to move toward a zone which is at higher pressure than the atmosphere.

The repeatability is excellent, with standard deviation of maximum penetration of less than 1.3 mm for all the conditions. (Fig. 3)

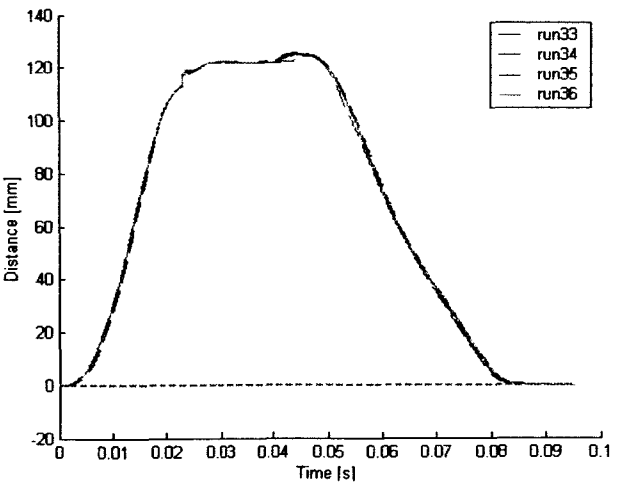

Figure 3. Performance comparison for several runs in the condition I (P=6 bar, Rod-Piston Weight=102.3 g, Pulse Delay1 = 0.015 s, Width Pulse1 = 0.035 s, Pulse Delay2 = 0.005 s, Width Pulse2 = 0.04 s)

Figure 4 shows a performance comparison pattern for the "old" run in nominal condition (P = 9 bar, Rod-Piston Weight = 102.3 g, Pulse Width = 0.115 s) and a "new" one (run n°35). The performance of the new TP configuration is vastly superior. In particular, the pressure inside the cylinder, for the same maximum penetration distance for the two injections, is decreased by 3 bar

while the flowtime is about one half the previous value. This characteristic permits us to provide us the possibility to obtain further air saving.

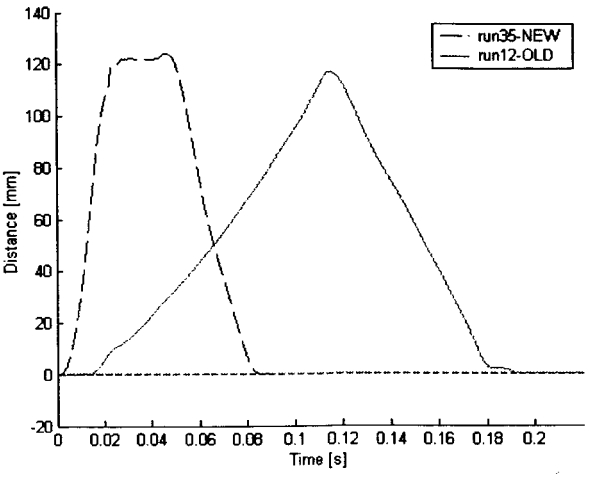

Figure 4. Performance comparison between an "old" run in the nominal condition (P = 9 bar, Rod-Piston Weight = 102.3 g, Pulse Width = 0.115 s) and a "new" run (P = 6 bar, Rod - Piston Weight = 102.3 g , Pulse Delay1 = 0.015 s, Width Pulse1 = 0.035 s, Pulse Delay2 = 0.005 s, Width Pulse2 = 0.04s)

Finally an important qualification has to be made: all of the injections were in atmospheric pressure; therefore some care has to be considered in extending the results to possible operations in Sesta were background pressure is well over 10 bar.

3.2.1 Performance w.r.t. rod weight

Figure 5 presents the influence of rod weight (conditions D, P, R) on the flowtime and maximum penetration performances (cylinder pressure = 4 bar). As expected, due to the higher inertia of the rod, as its weight increases, both the flowtime and the maximum penetration increase. The increased weight (added to simulate the performances of TP in the new configuration with the "new longer probe", see next section) allows a better injection performance and, at the same time, the flowtime is still really satisfactory (only 2 ms longer than the one obtained with no added weight).

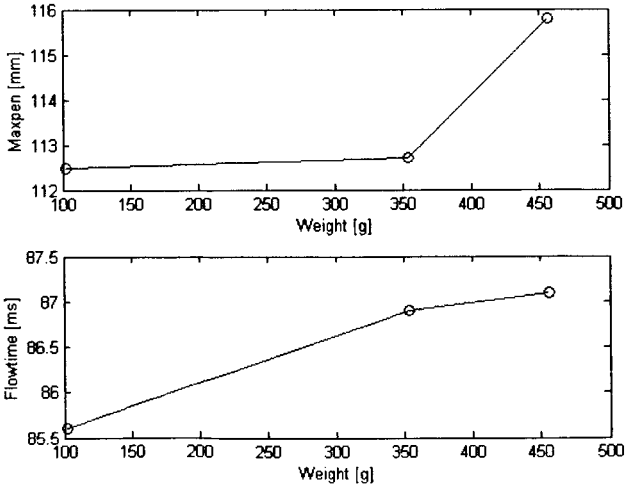

Figure 5. Weight influence on performance at P = 4 bar and at Pulse Delay1 = 0.015, Width Pulse1 = 0.035 s, Pulse Delay2 = 0.005 s, Width Pulse2 = 0.04 s (0.05 s) (flowtime in the upper plot, maximum penetration down)

Figure 6 shows the performance characteristics for the condition R. It is evident (see also Table 4) that the stationary time is particularly reduced, but it can be increased easily at will from the DAQ software interface.

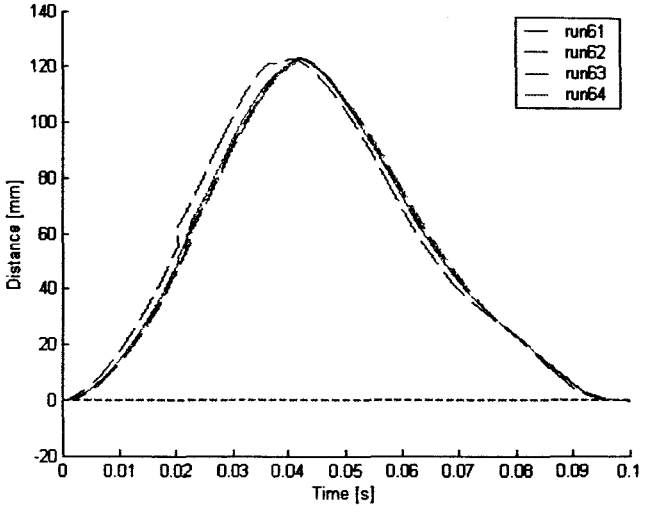

Figure 6. Performance comparison for several runs at the condition R (P = 4 bar, Rod - Piston Weight = 456.4 g, Pulse Delay1 = 0.015 s, Width Pulse1 = 0.035 s, Pulse Delay2 = 0.001 s, Width Pulse2 = 0.05 s)

3.2.2 Performance w.r.t. air pressure

Figure 5 presents the influence of cylinder pressure (conditions C, G, I) on the flowtime and maximum penetration performances (Rod-Piston Weight = 102.3 g).

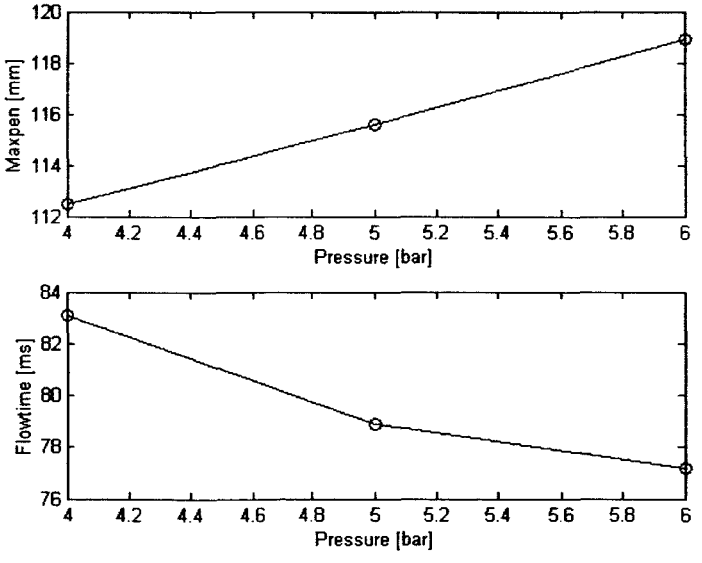

Figure 7. Pressure influence on performance with Pod-Piston Weight = 102.32 g and at Pulse Delay1 = 0.015 s, Width Pulse 1 = 0.035 s, Pulse Delay 2 = 0.005 s, Width Pulse 2 = 0.04 s (flowtime in the upper plot, maximum penetration down)

The maximum penetration increases linearly with pressure, while the flowtime decreases almost linearly. It is evident that the performances are totally satisfactory for all the 3 pressures and this allows the evaluation of the possibility of either improving the probe margin of safety or increasing the piston travel region.

4. New probe description

As previously mentioned, the probe design was considerably modified and is more complex than the probes used up to now separate pressure and temperature probes because it had to fulfil the following requirements:

- Simultaneous measurement of pressure and temperature fluctuations during the same run
- Measurement of pressure and temperature mean values (low frequency)
- Extraction of the probe from the back of the injection mechanism without having to remove anything else (quick substitution).

The first 2 requirements lead to a relatively high number of sensors (and therefore high number of wires coming out from the back of the injection mechanism) to be fitted in a relatively small space:

- 1 small size, miniature Kulite pressure transducer (model: XCQ-77-062-17BARA) (4 wires)
- 1 pitot tube
- 2 thin-film gauges with different substrates each: Coldierite and Quartz, the same used for the last experimental campaign (4 wires)
- 2 thermocouples: one fitted on the tip and the second one internal the probe (4 wires)

Figure 8 shows a scheme of the new sensor configuration on the probe, while Figure 9 shows the tip of the manufactured probe.

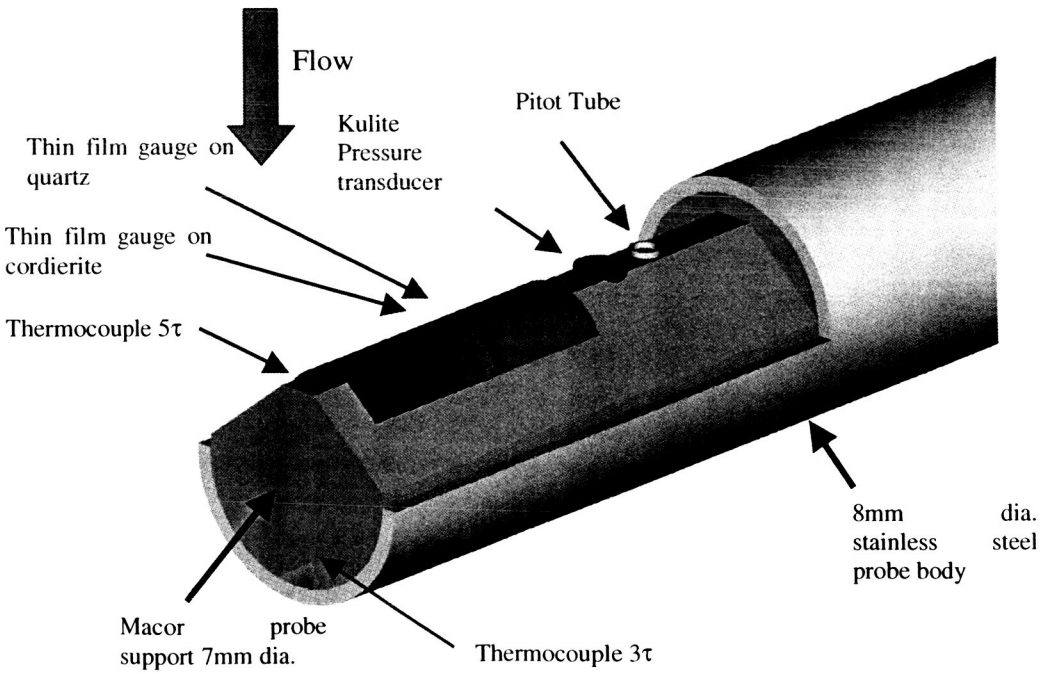

Figure 8. New probe scheme

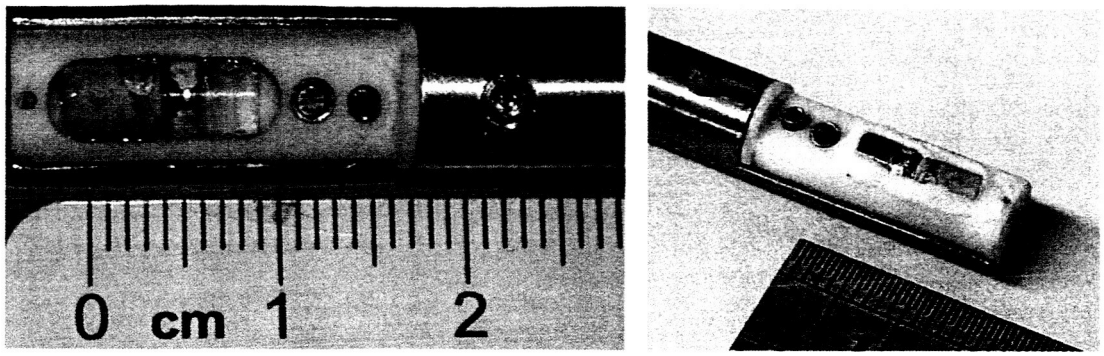

Figure 9. Photos of the manufactured probe. The left hand picture shows it during construction and the right hand shows the finished probe

In particular, the probe includes a self-heating two-substrate temperature probe, which recovers a heat flow total temperature by measuring the temperature histories of two thin film gauges, which start at the same temperature but reach different final temperatures due to the fact that are painted on different substrates.

One film is painted on a Quartz substrate and the other one on a Cordierite substrate (the same as used during the last experimental campaign); The thin films properties are presented in Table 5, while the film calibration is shown in Table 6.

Material	density, ρ (kg/m^3)	C (J/kgK)	k (W/mK)	ρ*c*k	sqrt(ρ*c*k)	Max Temp (°C)	diffusivity (m^2/s)
Quartz	2210.00	755.00	1.40	$2.34 \cdot 10^6$	1528.39	1200.00	$8.39 \cdot 10^{-7}$
Cordierite	2600.00	1464.40	3.00	$1.14 \cdot 10^7$	3379.69	1371.00	$7.88 \cdot 10^{-7}$

Tab. 5 Properties of Quartz and Cordierite

Material	Film Res. @ 20°C	Film Slope	Film alpha
Quartz	21.619	0.0312	$1.44*10^{-3}$
Cordierite	34.797	0.0594	$1.71*10^{-3}$

Tab. 6 Film calibration

In order to solve the problem of the "quick extraction" (the 3rd requirement) it was decided first to mount the 7 mm MACOR diameter body of the new probe, (green probe in Figure 10) inside a 8mm diameter Stainless Steel tube, (cyan tube in the next figure: the so called new probe-rod) connecting them through several screws and high temperature ceramic adhesive in order to withstand high pressure and temperature inside the test rig, and then to slide the new probe and probe-rod system inside a 10 mm diameter Stainless Steel piston rod. A Swagelock fitting at the end will be used to connect the piston rod and the probe rod.

It must be noted that this new configuration, more safe and efficient, required the re-design several parts of the injection mechanism, including an increase of the piston rod diameter from 9.5 mm to 10 mm. The new design will be presented in the last section.

As the leads are sealed into the probe tube, there is no need to have a separate feed through as used in the previous design. This considerably simplifies the process of connecting to the probe as no internal connections are required.

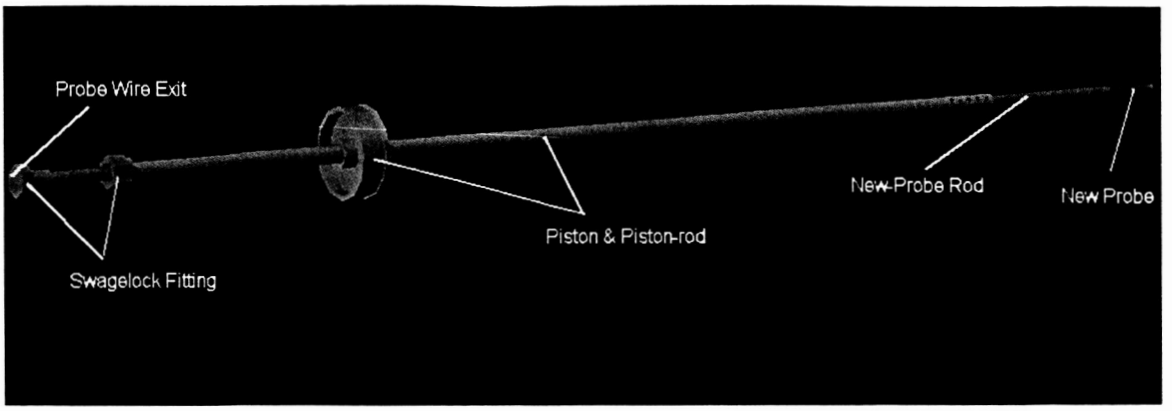

Figure 10. General scheme of the new fast-extracting probe

4.1 Calibration test description

The new probe was tested and calibrated at Oxford in collaboration with Oxford University and Centrospazio Space Research Laboratory, using the Oxford Step Heating Calibration Facility with a heat gun.

The facility trigger and the data acquisition system were controlled by the DAQ board installed on a standard PC computer through the use of software written in National Instrument's Labview 5.01 environment.

During the present experimental campaign the miniature Kulite pressure transducer and the two thermocouples were tested in order to estimate their correct signal responses while a more accurate experimental tests were conducted for calibrating the two thin film gauges.

The voltage thin films signals were acquired by the digital board, after passing through a pre-amplifier stage: a diffential input DC amplifier, an AC coupled amplifier and a low-pass antialiasing filter (the same amplifier system used for the last experimental tests). Before starting the experiments on the new probe, it was necessary to conduct several tests in order to verify the amplifier frequency response and to lower the noise level.

Figure 11 shows the frequency response comparison of the DC amplifier for the two thin film gauge channels. It is evident how the thin film gauge amplifier boosts the higher frequencies of the thin films gauges in order to reduce digitisation errors as the thin films voltage signal falls with the increasing frequency. The frequency responses are consistent with the amplifier design response.

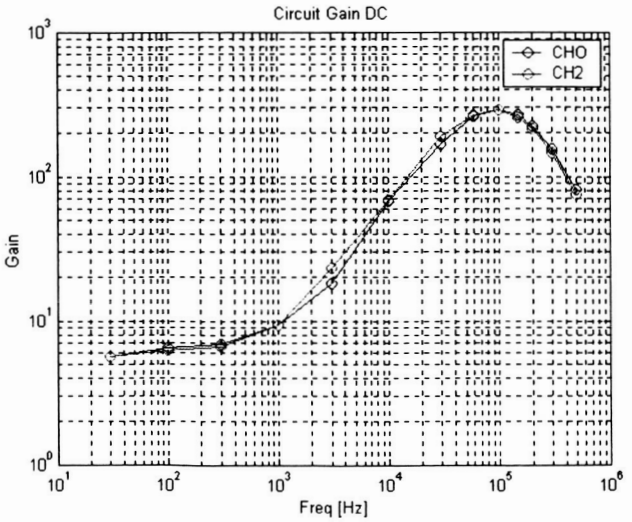

Figure 11. Frequency response comparison of the DC amplifier for the two thin film gauge channels

4.2 Calibration test results

This section presents the results obtained in Oxford in order to characterise the new probe design characteristics. After having set up all the instrumentations and data acquisition system as well as positioned correctly the probe under the heat gun flow, it was possible to begin the experimental campaign.

The thin films gauges were connected to two channels of the previously mentioned amplifier, one for the quartz film and one for the cordierite one. During the experiments, a constant current of 10 mA was maintained through the thin film gauges via a DC current supply in order to monitor the resistance changes with temperature variations for both thin films. The Post-processing routines were written in the Labview and Matlab environments.

Figure 12 shows the comparison between the temperature history for the two thin films.

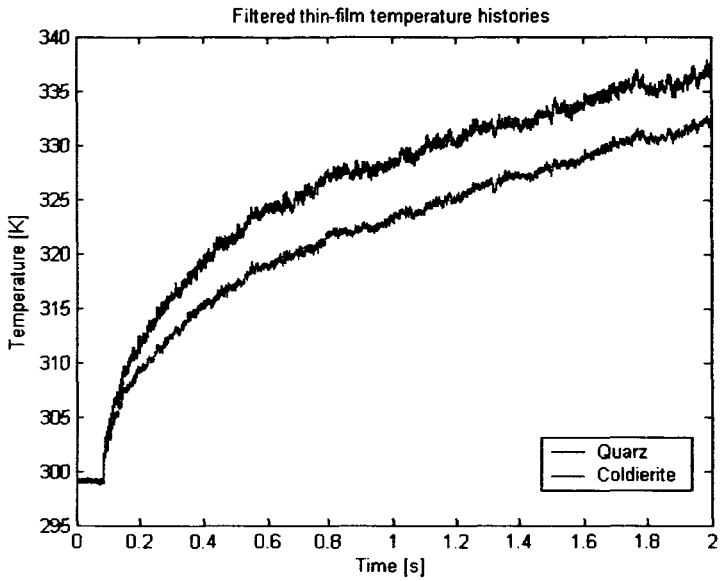

Figure 12. Comparison between the filtered temperature history for the two thin film for the run n°13 (Tin = 298°K, Time = 2sec, Sample rate = 250kHz).

It is evident from the above figure that there is a settling time at the beginning of the run due to the fact that films start at the same temperature.

The next figures presents the comparison between the heat flux history for the two thin films, and the flow total temperature history respectively.

To determine the heat flux history for the two films it was used the quasi-infinite substrate approximation and then the correcting formula [Buttsworth & Jones, 1997b] (1) for two-dimensional effects due to cylindrical shape of the probe (lateral conduction).

$$q = q_{1d} - \frac{k \cdot (T_{film} - T_{initial})}{D} \qquad (1)$$

The total temperature history was retrieved developing an iterative procedure which allows to determine h and the total temperature $Ttot$ ($q = h(Ttot - Tw)$). The fundamental hypothesis in this analysis assumes that the local flow around the probe is laminar; in this flow condition, the Nusselt and Reynolds numbers are connected by the relation $Nu \sim Re^{\frac{1}{2}}$, or $\frac{hd}{k} \sim \left(\frac{\rho V d}{\mu}\right)^{\frac{1}{2}}$, where

h, d, k, ρ, V and μ are heat transfer coefficient, probe diameter, thermal conductivity, gas density, flow velocity and gas viscosity respectively.

It is necessary to note that the aforementioned experiments were carried out only through the heat gun because it was not safe to expose the Kulite pressure transducer to the gas torch flow (which reach higher temperature than the heat gun) for several seconds. In this view, it is important to remember that the probe has to remain inside the rig, exposed to the hot flow, for only around 100 ms.

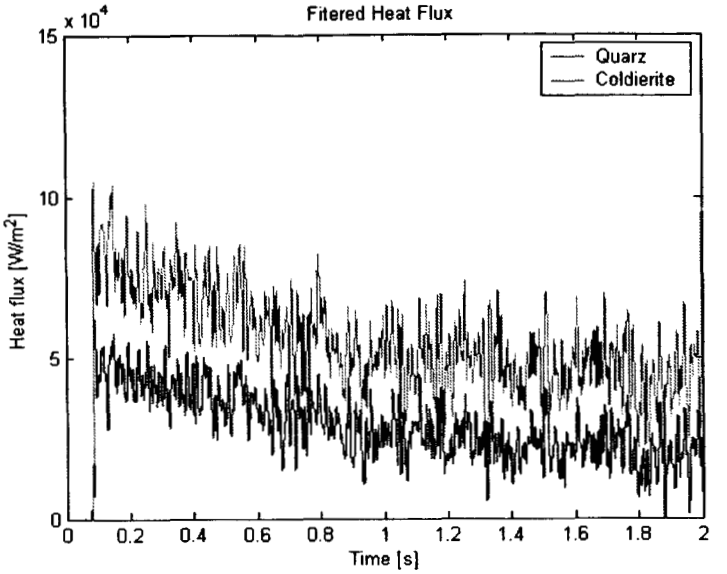

Figure 13. Comparison between the filtered heat flux history for the two thin film for the run n°13 (Tin = 298°K, Time = 2sec, Sample rate = 250kHz).

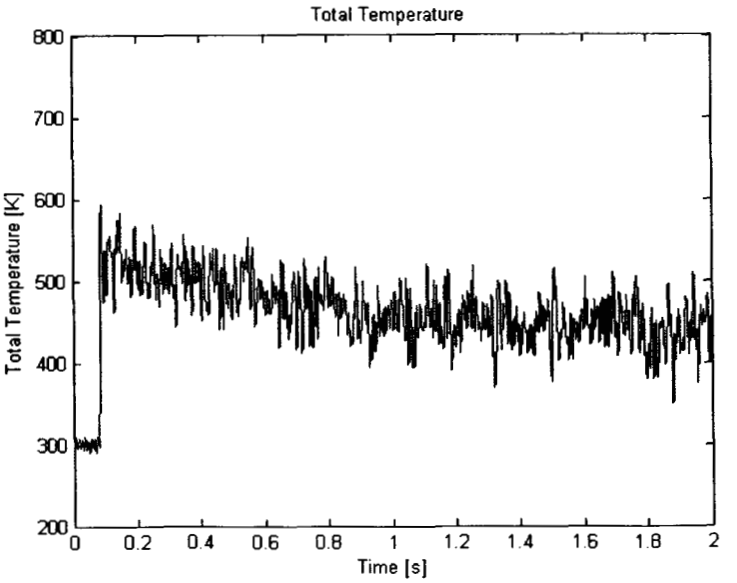

Figure 14. The total temperature history for the run n°13 (Tin = 298°K, Time = 2sec, Sample rate = 250kHz).

5. Sensing the temperature of the Kulite pressure transducer

Miniature Kulite pressure transducers, such as the XCQ-77-062-17BARA used in the new probe, use semiconductor resistive strain-sensors on the pressure sensitive diaphragm. Consequently

the resistance of the sensor between the constant supply voltage and the return earth lead is temperature dependent. Moss [4] showed that the temperature of the sensing elements could be measured by measuring the supply current of the Kulite sensor. This is very useful for health monitoring of the Kulite during insertion into the hot flow.

A new, simple, add-on operational amplifier circuit has been designed to measure the supply current without disturbing the constant 12 V supply voltage to the Kulite. One channel of the Kulite amplifiers is modified to enable this facility.

The XCQ-77-062-17BARA transducer has an input resistance of 2428 Ω, and so draws about 5.0 mA from a 12 volt supply. The current sensing circuit is designed to give an output of about +2.0 volts for this current, so as to suit a 0-5 V A/D. As designed, the circuit has a 10 kHz bandwidth. Figure 15 shows the add- on circuit.

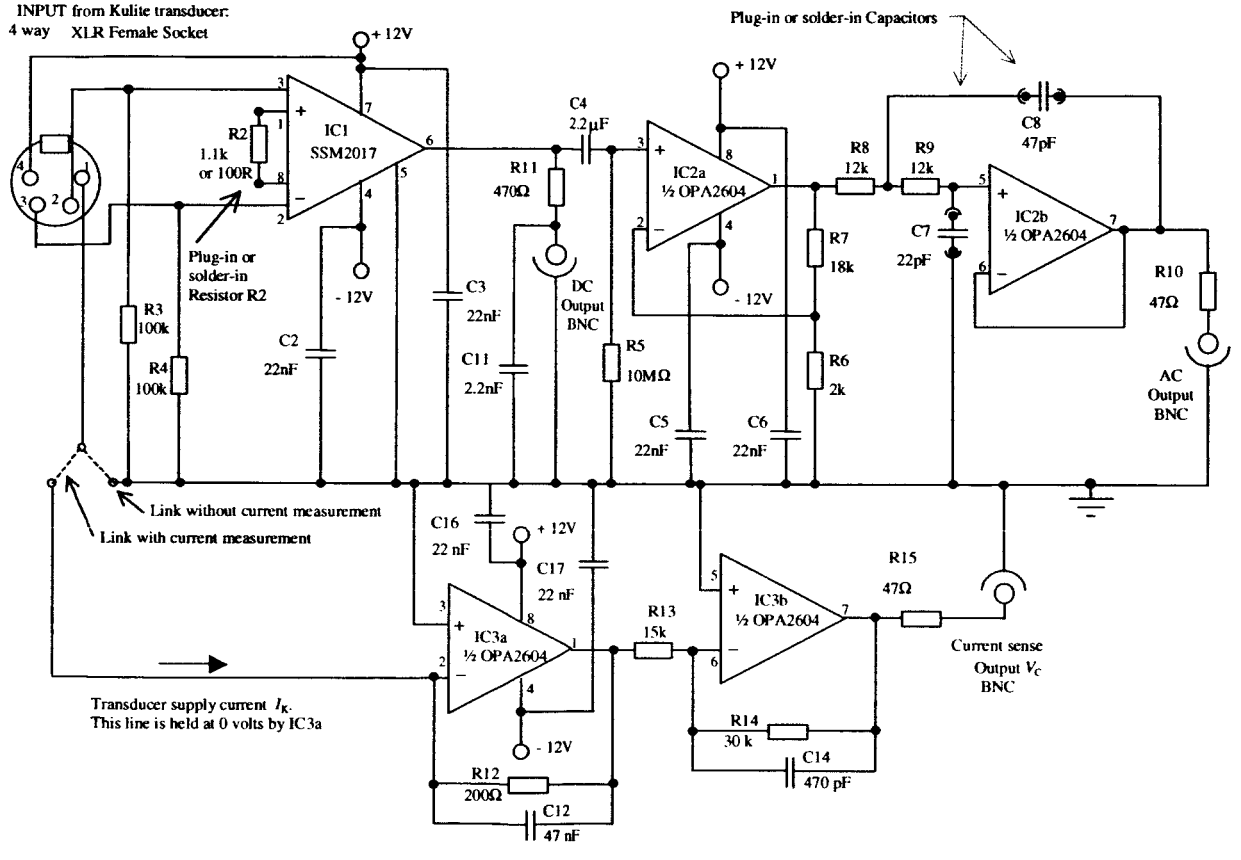

Figure 15. Pressure transducer supply current measuring circuit (IC3a & IC3b) added to the Pressure Transducer Signal Conditioning Unit.

6. Metric Turboprobe version

Figures 16 and 17 show a longitudinal cross-section of the Enel-Sesta test facility and, in particular, the position of the nozzle related to the old access port, used for carrying out the last experimental tests, as well as to the proposed new one, which could be utilized in the future experiments. Appendix A shows a transverse cross-section of new probe in Sesta working section.

Note that, the new access port allows the reduction of the probe distance from nozzle exit by about 300 mm in axial direction, but at the same time it requires an increase of the Turboprobe length in order to reach the centre of the rig (Appendix A).

In this view, some components (Table 7) of the Turboprobe mechanism have to be reconfigured in order to fulfil the new requirements. In particular, a new aspect is represented by the use of a new Stainless Steel-probe rod (that will slide inside it).

Due to that, we can note that in the worst case the weight of the rod-piston-probe system will be around 310 g (to that weight we have also to add the Swagelock connector, the instrumentations and the electrical cables weights).

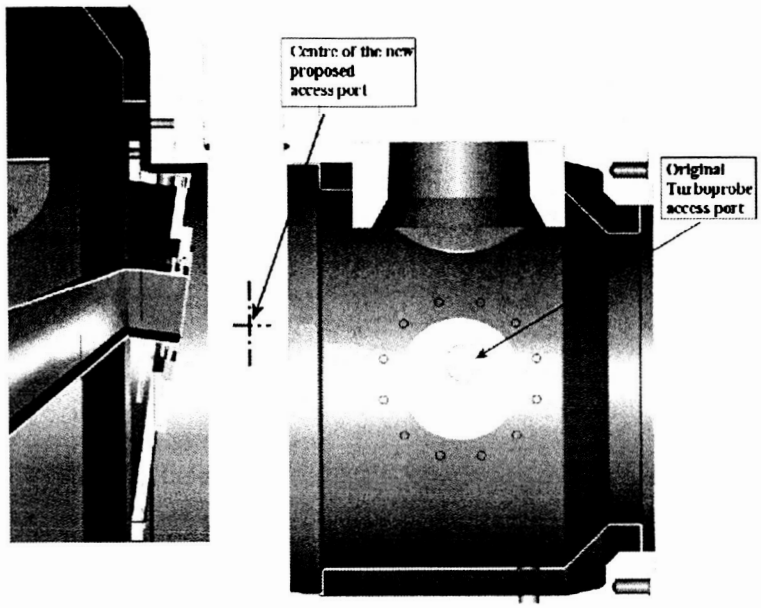

Figure 16. Schematic of the Sesta rig.

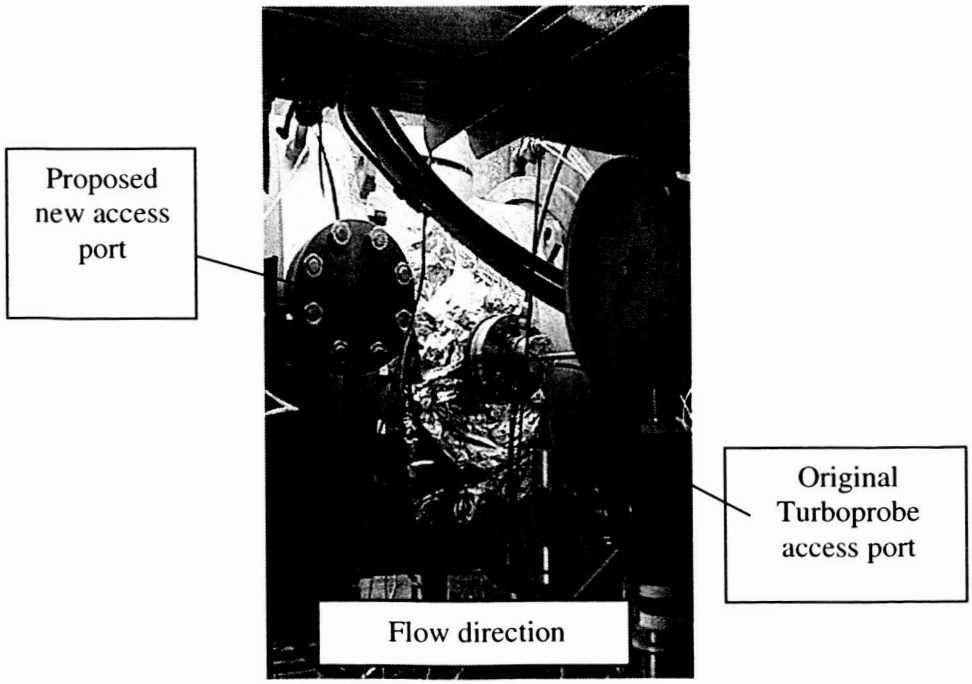

Figure 17. The new access port of Enel-Sesta facility.

	Material	Length (mm)	Inner Diameter (mm)	Outer Diameter (mm)	Weight (g)
Rod	AISI 1018	1100	9	10	127
Steel-Piston	AISI 1018	20	10	49	70
AL-Piston	AL 6061-T6	20	10	49	37
Probe	AISI 1018	1200	7	8	109

Table 7 . New injection mechanism components

Figure 18 shows the design of the Turboprobe (metric version), which will be mounted in the new access ENEL-Sesta port. It was necessary, in fact, to re-design all the injection mechanism in order to slide in it the new rod (in fact the old rod external diameter was 9.5 mm while the new one is 10 mm) and to have the TP in metric units. Figure 19 shows a photo of the assembly of the new manufactured Turboprobe.

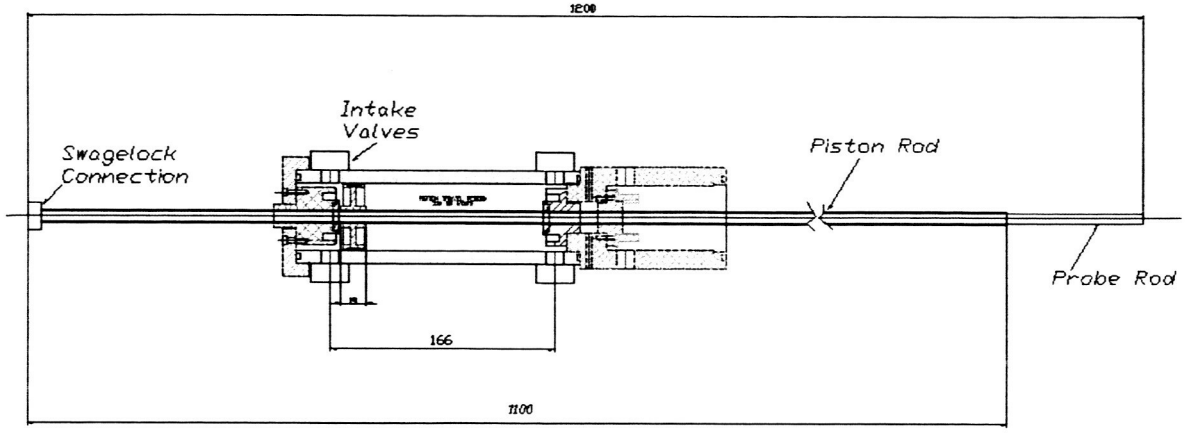

Metric Version

Figure 18. New Turboprobe mechanism configuration

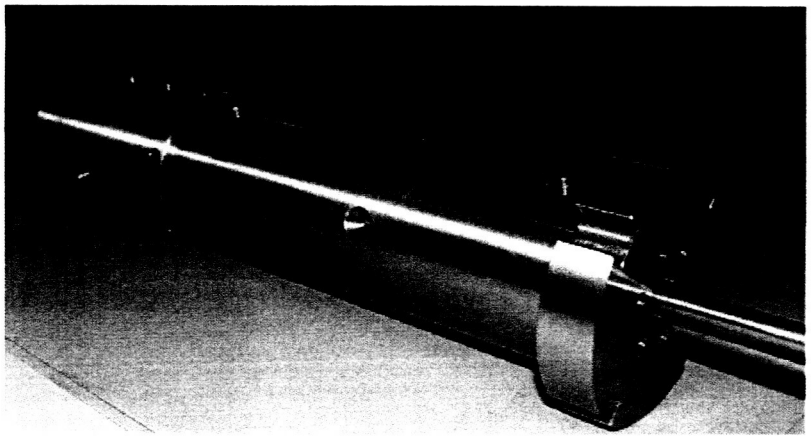

Figure 19. Photo of the new manufactured Turboprobe injection cylinder

6.1 Observation on piston-rod junction

The new injection mechanism was so powerful that the adhesive piston-rod join broke two times: the first one when the usual injection parameters were tested (nominal weight and 9 bar in the cylinder) and the second one when, after 250 runs, the tests were performed at higher pressure with an additional weight on the piston end. This means that other ways have to be examined to improve the join between the piston and the rod: the present adhesive connection is no longer

sufficient, because of the increased impact force of the piston on the springs/piston-stops (the injection speed is about 4 times bigger).

In order to solve this problem, it was decided to braze the stainless steel piston-rod to a stainless steel-piston, a better solution than using the aluminium-piston. Several tests have to be carried out in order to assure the safety of the junction.

Figure 20 presents the new piston design, while Figure 21 show the manufactured piston brazed to the stainless steel rod.

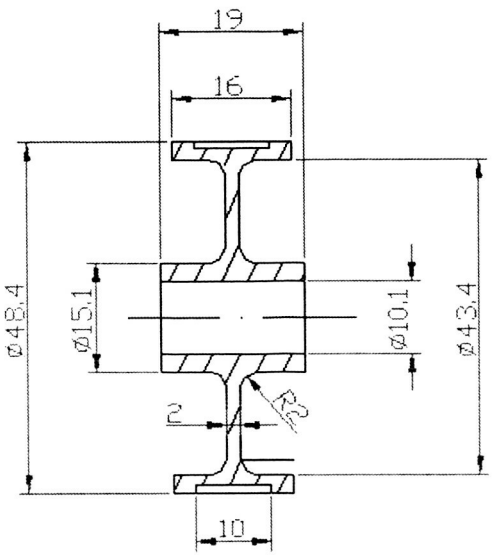

Figure 20. New piston design

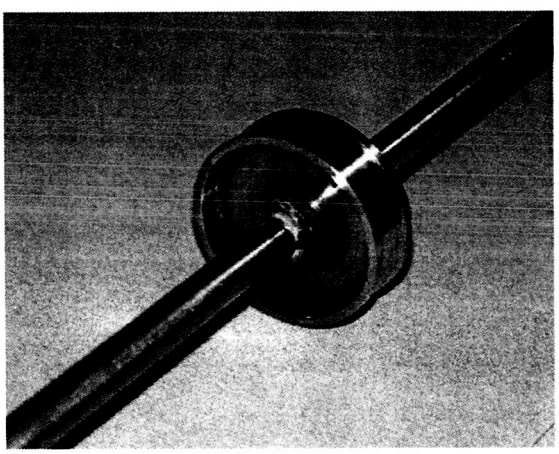

Figure 21. Photo of the new Stainless steel piston and rod

7. Conclusions

The activity for improving the performance characteristics of the present injection mechanism has been successful:

1. It was possible to control the solenoid valves separately through two different relays by the use of the DAQ board. This avoids a high rate of air consumption and therefore allows the possibility to use nitrogen bottles inside the rig. After 250 runs the air bottle consumption was only about 20% of bottle.
2. The injection performance is greatly improved: the probe immersion time is now less than one half of the one measured in the preceding runs (September 2002). At a cylinder pressure of 6 bar, the speed during the first phase (entry) is around 4.9 m/s

while during the second phase (exit) is around 3.5 m/s. This could lead to shorter injection time or increment injection distances.

3. The original requirements of 100 mm immersion distance in 100 ms are largely satisfied.
4. Modifications on probe geometry, including significant weight increase, didn't create problems with the injection mechanism. Sufficient penetration was obtained also with 4.5 times the present weight and the immersion kept low (around 70 ms) at a cylinder pressure of 4 bar.
5. A new type of probe was designed and manufactured in Oxford. Several sensors (2 thin films, 2 thermocouples, 1 pitot, 1 Kulite pressure transducer) were mounted on the same probe. The new probe was tested and calibrated in Oxford with the collaboration of Centrospazio Space Research Laboratory.
6. A simple circuit has been added to the Kulite pressure transducer amplifiers enabling the measurement of the current taken by the Kulite. This current is temperature dependant and will enable transducer diaphragm temperature to be monitored during a hot run.
7. The proposed new access port in the Enel test rig is closer to the actual combustor nozzle exit. There are some concerns over the increase in length of the probe (necessary because the new port is on a larger diameter part of the rig). It must be noted on the practical side that the new system will be much heavier than the original one, because of the more rugged stainless steel construction and the "quick extraction" system that allows removal of the probe without dismounting all the injection mechanism.
8. A new issue is posed by the increased impact force of the piston on the end stops, which broke two different adhesive piston-rod joints relatively easily. Some further testing is necessary to test the strength of the new brazed piston-to-rod joint in service.
9. The redesigned, more rugged injection mechanism and the new, easily removed multi-sensor probe have been successfully tested and will shortly be ready for use.

References

[1] Passaro A., LaGraff J, Oldfield M, Biagioni L, Moss R., Battelle R., 2003, – " *MEASUREMENT OF TURBULENT PRESSURE AND TEMPERATURE FLUCTUATIONS IN A GAS TURBINE COMBUSTOR*" Cleveland, 2003, NASA/Cr-2003-212540

[2] Battelle, R.T., 2001 – *"Design, Optimization and Testing of a Rapid Traversing Pressure Transducer for Measurement of Turbulent Spectra in a Gas Turbine Combustion Chamber"*, Master of Science Thesis, Syracuse University, 2001

[3] Buttsworth, D.R. and Jones, T.V., 1997, *"Radial Conduction Effects in Transient Heat Transfer Experiments"*, The Journal of the Royal Aeronautical Society, May 1997.

[4] Moss, R.W., 1992,"the Effects of turbulence Length Scale on Heat Transfer", D.Phil. thesis, Oxford University.

Appendix A

Cross-section of new probe in Sesta working section.